

 Open access • Posted Content • DOI:10.1101/2020.06.02.129296

Ecological Differentiation Among Globally Distributed Lineages of the Rice Blast Fungus *Pyricularia Oryzae* — [Source link](#)

Maud Thierry, Florian Charriat, Joëlle Milazzo, Henri Adreit ...+9 more authors

Institutions: ANSES

Published on: 28 Oct 2021 - bioRxiv (Cold Spring Harbor Laboratory)

Topics: Pyricularia

Related papers:

- [Congruent population genetic structures and divergence histories in anther-smut fungi and their host plants *Silene italica* and the *S. nutans* species complex](#)
- [Separation in flowering time contributes to the maintenance of sympatric cryptic plant lineages](#)
- [Genomic divergence in sympatry indicates strong reproductive barriers and cryptic species within *Eucalyptus salubris*.](#)
- [Deep sampling of ancestral genetic diversity reveals *Saccharomyces cerevisiae* pre-domestication life histories](#)
- [Niche differentiation and colonization of a novel environment by an asexual parasitic wasp](#)

Share this paper:    

View more about this paper here: <https://typeset.io/papers/ecological-differentiation-among-globally-distributed-143qx6dup8>

1 ECOLOGICAL DIFFERENTIATION AND INCIPIENT SPECIATION IN THE FUNGAL PATHOGEN CAUSING

2 RICE BLAST

3 Maud THIERRY^{1,2,3}, Florian CHARRIAT¹, Joëlle MILAZZO^{1,2}, Henri ADREIT^{1,2}, Sébastien RAVEL^{1,2},
4 Sandrine CROS-ARTEIL¹, Sonia BORRON¹, Violaine SELLA³, Thomas KROJ¹, Renaud IOOS³, Elisabeth
5 FOURNIER¹, Didier THARREAU^{1,2,4}, Pierre GLADIEUX^{1,4}

6 ¹PHIM Plant Health Institute, Univ Montpellier, INRAE, CIRAD, Institut Agro, IRD, Montpellier, France

7 ²CIRAD, UMR PHIM, 34090 Montpellier, France.

8 ³ANSES Plant Health Laboratory, Mycology Unit, Domaine de Pixérécourt, Bâtiment E, F-54220 Malzéville,
9 France

10 ⁴pierre.gladieux@inrae.fr; didier.tharreau@cirad.fr

11 **ABSTRACT**

12 Many invasive fungal species coexist as multiple populations on the same host, but the factors behind
13 the origin and maintenance of population structure remain largely unknown. Here, we analyzed
14 genetic and phenotypic diversity in isolates of the rice blast fungus (*Pyricularia oryzae*) covering a
15 broad geographical range. We showed that the four lineages of *P. oryzae* were found in areas that
16 differ in terms of prevailing environmental conditions and types of rice grown. Pathogenicity tests
17 revealed that specialization to rice subspecies contributed to niche separation between lineages, and
18 differences in repertoires of putative pathogenicity effectors were consistent with differences in host
19 range. Crossing experiments revealed that female sterility and early post-mating genetic
20 incompatibilities acted as strong barriers to gene flow between these lineages. Our results
21 demonstrate that the spread of a pathogen across heterogeneous habitats and divergent populations
22 of a crop species can lead to niche separation and incipient speciation.

23 Short title: Incipient speciation in the rice blast pathogen

24

25 INTRODUCTION

26 Understanding and controlling natural variation in fungal plant pathogens is of great importance for
27 maintaining food security and ecosystem health. In addition to the overwhelming phylogenetic
28 diversity of pathogens (Burdon 1993), many pathogens also harbor substantial diversity at the species
29 scale (Taylor & Fisher 2003). Most fungal pathogens of plants form distinct populations (Taylor *et al.*
30 2006), and this population structure is a compound outcome of migration, selection and drift, acting
31 at multiple scales, and patterned by factors such as time (Ali *et al.* 2014; Pagliaccia *et al.* 2018),
32 admixture (Robert *et al.* 2015), geography (Ali *et al.* 2014; Marin *et al.* 2009; Yang *et al.* 2018), mode
33 of reproduction (Ali *et al.* 2014; Bueker *et al.* 2016; Gibson *et al.* 2012; Ropars *et al.* 2016) and
34 environmental conditions (Walker *et al.* 2015). The identity of the host plants with which fungal
35 pathogens interact is widely thought to be the environmental factor structuring the pathogen
36 population with the strongest impact. Many plant pathogens reproduce within or on their host,
37 resulting in assortative mating on the basis of host use and a strong association between adaptation
38 to the host and reproductive isolation (Giraud *et al.* 2010; Servedio *et al.* 2011). However, more
39 generally, population structure can result from limited dispersal (i.e. limited gene flow due to
40 distance) or limited adaptation (i.e. limited gene flow because of differences in the capacity to exploit
41 resources), both of which may be due to a wealth of potential factors largely unexplored in plant
42 pathogens. Developing an understanding of how population structure emerges and is maintained in
43 fungal plant pathogens is a major goal in evolutionary microbiology, because it will improve our
44 comprehension of both disease emergence and the origin of fungal biodiversity.

45 *Pyricularia oryzae* (Ascomycota; syn. *Magnaporthe oryzae*) is a widespread model plant
46 pathogen displaying population subdivision. Several lineages, each associated mostly with a single
47 main cereal/grass host, have been characterized within *P. oryzae* (Gladieux *et al.* 2018a). The lineage
48 infecting Asian rice (*Oryza sativa*) has been characterized in detail. Previous population genomic
49 studies of population structure in the rice-infecting lineage revealed genetic subdivision into three
50 (Saleh *et al.* 2014; Tharreau *et al.* 2009; Zhong *et al.* 2018) to six (Gladieux *et al.* 2018b) lineages,

51 estimated to have diverged approximately 1000 years ago (Gladieux *et al.* 2018b; Latorre *et al.* 2020;
52 Zhong *et al.* 2018). *Pyricularia oryzae* is a heterothallic fungus with a sexual cycle involving mating
53 between individuals of opposite mating types, with at least one of the partners capable of producing
54 female structures (i.e. “female-fertile”). One single lineage (lineage 1, prevailing in East and Southeast
55 Asia) displayed a genome-wide signal of recombination, a balanced ratio of mating type alleles and a
56 high frequency of fertile females, consistent with sexual reproduction (Gladieux *et al.* 2018b; Saleh *et al.*
57 2014; Saleh *et al.* 2012b). All the other lineages had clonal population structures, highly biased
58 frequencies of mating types and few fertile females, suggesting strictly asexual reproduction
59 (Gladieux *et al.* 2018b; Saleh *et al.* 2014). In theory, gene flow remains possible between the majority
60 of the lineages, because there are rare fertile strains and some lineages have fixed opposite mating
61 types. However, while resequencing studies have revealed signatures of recent shared ancestry
62 between clonal lineages and the recombinant lineage from South-West Asia, this is not the case
63 between the different clonal lineages, consistent with a lack of recent gene flow between lineages of
64 opposite mating types and despite their wide and overlapping distributions (Gladieux *et al.* 2018b).
65 The loss of female fertility is probably a key factor in the emergence of clonal lineages, inducing a
66 shift towards strictly asexual reproduction, and protecting populations adapting to new conditions
67 from maladaptive gene flow from ancestral, recombining populations (Giraud *et al.* 2010). This raises
68 questions about the nature of the factors underlying the emergence of different rice-infecting
69 lineages in *P. oryzae*, and contributing to their maintenance, because, according to the competitive
70 exclusion principle, different lineages should not be able to co-exist on the same host (Abbate *et al.*
71 2018; Giraud *et al.* 2017; Hardin 1960). Previous studies have helped to cement the status of *P. oryzae*
72 as a model for studies of the population biology of fungal pathogens, but most efforts to understand
73 the population structure of the pathogen have been unable to provide a large-scale overview of the
74 distribution of rice-infecting lineages and of the underlying phenotypic differences, because the
75 number of genetic markers was limited (Saleh *et al.* 2014; Tharreau *et al.* 2009), the number of

76 isolates was relatively small (Gladieux *et al.* 2018b; Zhong *et al.* 2018) and because few phenotypic
77 traits were scored (Saleh *et al.* 2014; Tharreau *et al.* 2009; Zhong *et al.* 2018).

78 We provide here a detailed genomic and phenotypic overview of natural variation in rice-
79 infecting *P. oryzae* isolates sampled across all rice-growing areas of the world. With a view to
80 inferring and understanding the global population structure of rice-infecting *P. oryzae*, we analyzed
81 genetic variation, using genotyping data with a high resolution in terms of genomic markers and
82 geographic -coverage, and measured phenotypic variation for a representative subset of the sample
83 set. We also characterized the genetic variability and content of repertoires of effectors –secreted
84 proteins that modulate host responses – using whole-genome resequencing data for a representative
85 set of isolates. We addressed the following specific questions: (i) How many different lineages of *P.*
86 *oryzae* infect rice? (ii) Do lineages of *P. oryzae* display footprints of recombination? (iii) Do lineages of
87 *P. oryzae* present evidence of recent admixture? (iv) Are the different lineages sexually competent
88 and compatible? (v) Are the different lineages differentially adapted to host and temperature? (vi)
89 Can we find differences in number, identity and molecular evolution of putative effectors between
90 lineages? (vii) Can we find differences in the geographic and climatic distribution of lineages?

91 **RESULTS**

92 **The rice blast pathogen comprises one recombining, admixed lineage and three clonal, non-**
93 **admixed lineages**

94 We characterized the global genetic structure of the rice blast pathogen, using an Illumina genotyping
95 beadchip to score 5,657 SNPs distributed throughout the genome of 886 *P. oryzae* isolates collected
96 from cultivated Asian rice in 51 countries (Supplementary file 1). The final dataset included 3,686
97 SNPs after the removal of positions with missing data, which identify 264 distinct multilocus
98 genotypes out of 886 isolates. Clustering analyses based on sparse nonnegative matrix factorization
99 algorithms, as implemented in the sNMF program (Frichot et al., 2014), revealed four clusters,
100 hereafter referred to as “lineages” (Figure 1C). The model with $K=4$ clusters was identified as the best
101 model on the basis of the cross-entropy criterion, as models with $K>4$ induced only a small decrease
102 in cross-entropy, suggesting that $K=4$ captured the deepest subdivisions in the dataset (Figure 1 –
103 figure supplement 1). The neighbor phylogenetic network inferred with SPLITSTREE also supported the
104 subdivision into four widely distributed lineages, with long branches separating three peripheral
105 lineages branching off within a central lineage (Figure 1A; 1B). A comparison with previous findings
106 revealed that the central lineage corresponded to the combination of recombining lineage 1 and
107 lineages 5 and 6, represented by two and one individuals, respectively, in (Gladieux *et al.* 2018b)
108 (Supplementary file 2). This central lineage is referred to hereafter as lineage 1. The three peripheral
109 lineages in the network corresponded to the previously described lineages 2, 3 and 4 (Gladieux *et al.*
110 2018b) with lineages 2 and 3 similar to lineages B and C, respectively, identified on the basis of
111 microsatellite data in a previous study (Saleh *et al.* 2014)(Supplementary file 2). Genetic
112 differentiation between the four lineages was strong and significant (Weir and Cockerham’s $F_{ST}>$
113 0.54), indicating strong barriers to gene flow between the lineages. All genotypes from lineages 2 to 4
114 had high proportions of membership q in a single cluster ($q > 0.89$), whereas shared ancestry with the
115 other three lineages was detected in lineage 1, with 32% of genotypes having $q > 0.10$ in lineages 2-4

116 (Figure 1C; Figure 1 – source data 3). Admixture may account for the lower F_{ST} observed in
117 comparisons between lineage 1 and the other lineages. We detected no footprints of recombination
118 in lineages 2, 3 and 4 with the pairwise homoplasmy index (PHI) test and a null hypothesis of clonality
119 (Table 1), confirming previous findings (Gladieux *et al.* 2018b; Latorre *et al.* 2020; Saleh *et al.* 2014;
120 Zhong *et al.* 2018).

121

122 **Geographic structure and admixture within recombining lineage 1**

123 Lineage 1 was the only lineage for which there was population genetic evidence of recombination in
124 the PHI test (Table 1). Most of the lineage 1 isolates were collected in Asia (79%), but the lineage was
125 present in all continents in which the pathogen was sampled (Europe: one isolate; North America: 10,
126 Central and South America: 7, Africa: 22) (Figure 2). Clustering analysis on this single lineage with
127 sNMF detected four clusters with different geographic distributions (Figure 2). Estimates of
128 differentiation were lower between the clusters within lineage 1 ($F_{ST} < 0.49$) than between the main
129 lineages ($F_{ST} > 0.54$), consistent with a longer history of restricted gene flow between the main
130 lineages and a more recent history of admixture between clusters within lineage 1 (Supplementary
131 file 3; Figure 1C).

132 Two clusters within lineage 1 (referred to hereafter as *Baoshan* and *Yule*) consisted mostly of
133 isolates sampled from two different sites in the Yunnan province of China (Baoshan and Yule,
134 respectively, located about 370 km apart). The third cluster consisted mostly of isolates from Laos
135 and South China (referred to hereafter as *Laos*), and the fourth brought together 95% of the isolates
136 from lineage 1 collected outside Asia (referred to hereafter as *International*). In Asia, the *International*
137 cluster was found mostly in the Yunnan province of China, India and Nepal (Figure 2). PHI tests for
138 recombination rejected the null hypothesis of clonality in all four clusters (Table 1). Admixture was
139 widespread in lineage 1 (Figure 2), with most of the isolates (78%) displaying membership
140 proportions $q > 0.10$ for two or more clusters (Figure 2). Only five genotypes were detected in
141 multiple countries (genotype ID [number of countries]: 2 [6], 18 [2], 58 [2], 98 [3] and 254 [3],

142 corresponding to 41 isolates in total). All these genotypes belonged to the *International* cluster.

143

144 Table 1. PHI test for recombination (null hypothesis: clonality) and distribution of mating types and fertile females in
145 lineages, and in clusters within lineage 1. PHI tests were carried out using source files Figure 1 – source data 1 and Figure 2 –
146 source data 1. Information about mating types and female fertility is available in Supplementary file 1.

Lineage/Cluster	p-value PHI test	Mat1.1/Mat1.2 (%)	Female-fertile isolates (%)
1	<0.0001	53/47	43
<i>Baoshan</i>	<0.0001	69/31	67
<i>International</i>	<0.0001	55/45	4
<i>Laos</i>	<0.0001	68/32	37
<i>Yule</i>	<0.0001	40/60	79
2	0.25	97/3	0
3	0.18	3/97	7
4	0.22	97/3	0

147

148 **Reproductive barriers caused by female sterility and postmating genetic incompatibilities**

149 Our analysis of genotyping data revealed the existence of a large, ancient, recombinant population
150 from which several clonal lineages have more recently emerged. This raised the question as to why
151 these populations became clonal, with no further gene flow. We addressed this question by
152 determining the capacity of the different lineages to engage in sexual reproduction, by characterizing
153 the distribution of mating types and the ability to produce female structures (i.e. female fertility).
154 Using *in vitro* crosses with tester strains, we found that lineages 2, 3 and 4 were composed almost
155 exclusively of a single mating type (97% of lineage 2 and 4 isolates tested carried the *Mat1.1* allele;
156 97% of lineage 3 isolates carried the *Mat1.2* allele), and had only small proportions (0-7%) of isolates
157 with female fertility (Table 1). By contrast to these clonal lineages, the mating type ratio was more
158 balanced in lineage 1 (52% of *Mat1.1*; Table 1), with *Mat1.1/Mat1.2* ratios ranging from 40/60 in the
159 *Yule* cluster to 69/31 in the *Baoshan* cluster. Female fertility rates were higher in three of the clusters
160 in lineage 1 (*Yule*: 79%; *Baoshan*: 67%; *Laos*: 37%; Table 1), but that in the *International* cluster (4%

161 female fertility) was as low as those in the clonal clusters (Table 1). These observations indicate that
162 there is a potential for sexual reproduction between lineages with compatible mating types and,
163 albeit rare, fertile females, but not between lineages 2 and 4, due to the low female fertility rates
164 and highly biased mating type ratios.

165 We further assessed the likelihood of sexual reproduction within and between lineages, by
166 evaluating the formation of sexual structures (perithecia), the production of asci (i.e. meiotic octads
167 within the perithecia) and the germination of ascospores (i.e. meiospores in meiotic octads) in
168 crosses between randomly selected isolates of opposite mating types from all four lineages (Figure 3).
169 This experiment revealed a marked heterogeneity in the rate of perithecium formation across
170 lineages. Three clusters in lineage 1 had the highest rates of perithecia formation, with isolates in the
171 *Yule* cluster, in particular, forming perithecia in 93% of crosses with isolates from the same cluster,
172 and in more than 46% of crosses with isolates from other lineages (Figure 3A). Isolates from lineages
173 2, 3 and 4 could only be crossed with isolates from other lineages, given their highly biased mating
174 type ratios, and the percentage of these crosses producing perithecia was highly variable (ranging
175 from 0% to 83%, depending on the lineages involved; Figure 3A). The rate of perithecium formation
176 was similar in crosses involving the *International* cluster of lineage 1 and in crosses involving clonal
177 lineages 2-4, and none of the crosses attempted between isolates from the *International* cluster led
178 to perithecium formation (Figure 3A). Perithecium dissection for a subset of crosses involving some of
179 the most fertile isolates revealed that most inter-lineage crosses produced perithecia that did not
180 contain asci or contained asci with low ascospore germination rates (Figure 3B). Whereas 100% of
181 crosses between isolates of the *Yule* cluster produced numerous germinating ascospores, ascospore
182 germination rates were only 33%, 56% and 7% in *Yule* x lineage 2, *Yule* x lineage 3 and *Yule* x lineage 4
183 crosses, respectively. Together, these results indicate that the clonal structure of lineages 2-4 is
184 caused by highly biased mating types and female sterility, and that the three clonal lineages and the
185 *International* cluster of lineage 1 are isolated from each other by strong pre- and early-postmating
186 barriers, including breeding system isolation (differences in mating type and female sterility), and a

187 combination of gametic incompatibility, zygotic mortality or hybrid non-viability. However, three of
188 the clusters in lineage 1 had biological features consistent with an ability to reproduce sexually,
189 suggesting possible sexual compatibility with clonal lineages 2-4 and the *International* cluster.

190 **Specialization to temperature conditions and rice subspecies**

191 Specialization can further reduce gene flow, and may facilitate niche separation between lineages,
192 which should favor the emergence of new lineages and their maintenance on the same host species
193 in conditions of competitive exclusion. The strong reproductive barriers demonstrated in our analysis
194 of crossing experiments would favor the establishment of such specialization, because reproductive
195 isolation facilitates adaptation to new conditions, by preventing maladaptive gene flow from
196 ancestral, non-adapted populations (Giraud *et al.* 2010). Given the very broad distribution of *P.*
197 *oryzae* and the strong environmental heterogeneity with which it is confronted in terms of the
198 nature of its hosts and the climate in which it thrives, we evaluated the variation of pathogen fitness
199 over different types of rice and temperature conditions.

200 We measured growth rate and sporulation rate of representative isolates cultured at different
201 temperatures to test the hypothesis of adaptation to temperature. Experiments were conducted with
202 41 isolates (lineage 1 [yule cluster]: 11; lineage 2: 10; lineage3: 10; lineage 4: 10). For all lineages,
203 mycelial growth rate increased with incubation temperature, although this trend was more visible
204 from 10°C to 15°C (increased mean mycelial growth of +2.22 mm/day) than from 25°C to 30°C (+0.05
205 mm/day) (growth curves and full statistical treatment of data are presented in Supplementary file 4;
206 data are reported in Supplementary file 5). Fitting a linear mixed-effects model with incubation time,
207 experimental replicate, and lineage of origin as fixed effects and isolate as a random effect, revealed a
208 significant lineage effect at each incubation temperature [10°C: $F(1,364)=7988$, $p<0.001$; 15°C:
209 $F(1,419)=33161$, $p<0.001$; 20°C: $F(1,542)=40335$, $p<0.001$; 25°C: $F(1,413)=30156$, $p<0.001$; 30°C:
210 $F(1,870)=52681$, $p<0.001$]. Comparing least-squares means resulting from linear mixed-effects
211 models at each temperature revealed a significantly lower growth rate of lineage 4 at 10°C compared

212 to other lineages and a significantly higher growth rate of lineage 1 at 15°C, 20°C, 25°C and 30°C
213 compared to other lineages. As regards sporulation rates, sporulation was nearly absent at 10°C after
214 20 days of culture, with the few spores observed being not completely formed and divided by only
215 one septum instead of two septa in mature conidia (sporulation curves and full statistical treatment
216 of data are presented in Supplementary file 6; data are reported in Supplementary file 7). For all
217 lineages, sporulation rates increased with temperature from 15 to 25 °C and dropped at 30°C,
218 although isolates were cultured 7 days only at this latter temperature instead of 10 days at other
219 temperatures. Isolates were cultured 7 days only at 30°C because at this stage the mycelium had
220 reached the edges of the plates. Significant lineage effects were observed at 10°C, 15°C and 30°C
221 (Kruskal-Wallis tests; 10°C: $H(3)=9.61$, $p=0.022$; 15°C: $H(3)=16.8$, $p<0.001$; 30°C: $H(3)=8.96$, $p=0.030$).
222 Pairwise non-parametric comparisons using Dunn's test of lineages revealed significant differences
223 between lineages 1 and 2 at 10°C, between lineage 1 and lineages 3 and 4 at 15°C, and between
224 lineage 1 and 4 at 30°C. Together, measurements of mycelial growth and sporulation at different
225 temperatures revealed differences in performance between lineages, but no clear pattern of
226 temperature specialization.

227 We assessed the importance of adaptation to the host, by challenging 45 rice varieties
228 representative of the five main genetic groups of Asian rice (i.e. the temperate japonica, tropical
229 japonica, aus, aromatic and indica subgroups of *Oryza sativa*) with 70 isolates representative of the
230 four lineages of *P. oryzae* and the four clusters within lineage 1 (Supplementary file 8). Interaction
231 phenotypes were assessed qualitatively by scoring resistance (from full to partial resistance: scores 1
232 to 3) or disease symptoms (from weak to full susceptibility: scores 4 to 6) and analysed by fitting a
233 proportional-odds model, followed by an analysis of variance (full statistical treatment of data is
234 presented in Supplementary file 9). This analysis revealed significant differences between groups of
235 isolates ($\chi^2(6)=100$, $p<0.001$), and between rice genetic groups ($\chi^2(4)=161$, $p<0.001$), and a significant
236 interaction between these two variables ($\chi^2(24)=97$, $p<0.001$). The finding of a significant interaction
237 between groups of isolate (lineage or cluster) and rice types indicates that the effect of the group of

238 isolates on the proportion of compatible interactions differed between rice types, suggesting
239 adaptation to the host. This is also supported by the specific behaviour of certain lineages. Isolates
240 from lineage 2 showed e.g. much lower symptom scores than the other lineages on all rice types
241 except temperate japonica and the isolates of the *Yule* cluster possess particularly high virulence on
242 indica varieties (Figure 4A; Supplementary file 8). In comparisons of rice genetic groups, significantly
243 higher symptom scores were observed on temperate japonica rice than on the other types of rice,
244 whereas the varieties of the aromatic genetic group were significantly more resistant to rice blast
245 (Figure 4B). Together, these experiments therefore revealed significant differences in host range
246 between lineages, but this specialization to the host is not strict since host ranges overlap (Figure 4C-
247 G). Adaptation to the host or small differences in temperature optima could, nonetheless, further
248 increase niche separation and reduce gene flow between lineages, via pre-mating barriers such as
249 immigrant non-viability (i.e., lower rates of contact between potential mates due to the mortality of
250 immigrants; (Gladieux *et al.* 2011; Nosil *et al.* 2005)), and post-mating barriers, such as ecological
251 hybrid non-viability (i.e., lower survival of ill-adapted hybrid offspring).

252 **Differences in number and genetic variability of putative effector genes among *P. oryzae* lineages**

253 Small secreted proteins named effectors are the most prominent class of fungal virulence factors.
254 They act by manipulating host cellular pathways and are key determinants of the host range and
255 fitness on compatible hosts (Liao *et al.* 2016; Yoshida *et al.* 2016). We therefore determined the
256 differences of effector repertoires in *P. oryzae* lineages in terms of presence/absence and nucleotide
257 polymorphism, and analyzed whether it is a particularly dynamic fraction of the gene space. For this
258 aim, we used whole-genome sequencing data for 123 isolates, including 29 isolates sequenced in this
259 study and 94 publicly available genomes (Gladieux *et al.* 2018a; Pordel *et al.* 2020; Zhong *et al.* 2018),
260 of which 33 were also genotyped using our Infinium genotyping beadchip (Supplementary file 10;
261 Appendix 1). Clustering analysis indicated that this dataset covered the four lineages of *P. oryzae*, and
262 three of the clusters of lineage 1 (Laos, International and Baoshan; Appendix 1; Supplementary file

263 10). Assembly lengths for the 123 sequenced isolates varied from 36.7 to 39.6 Mb, with an average of
264 38.1 Mb (Supplementary file 10). The number of assembled contigs longer than 500bp ranged from
265 1010 to 2438, and the longest contig was 1.1 Mb (Supplementary file 10).

266 Gene prediction identified 11,684 to 12,745 genes per genome, including 1,813 to 2,070
267 genes predicted to code for effector proteins. We found a significant effect of the lineage of origin on
268 both the mean number of putative effector genes (ANOVA, $F=5.54$, $p=0.0014$), and the mean number
269 of non-effector genes (ANOVA, $F=7.95$, $p<0.001$). Multiple comparisons revealed that mean numbers
270 of putative effectors and non-effector genes were only significantly different between genomes of
271 lineage 3 and lineages 2 (Tukey's HSD test; $p<0.001$; Supplementary file 11). Orthology analysis
272 identified 14,573 groups of orthologous sequences (i.e. orthogroups), and we applied a rarefaction
273 approach to the table of orthology relationships to estimate the size of accessory and core genomes
274 in lineages while accounting for differences in sample size. For both putative effectors and the
275 remaining of the gene space, we found that the number of core and accessory genes did not plateau
276 and changed almost linearly with the number of genomes resampled, indicating that the number of
277 core genes is likely substantially smaller, and the number of accessory genes substantially higher, than
278 estimated from 123 genomes (Supplementary file 12). With pseudo-samples of size $n=30$ per lineage
279 (i.e. excluding lineage 4, due to small sample size), the gene content was highly variable within
280 lineages with only 61-71% of all predicted effectors, and 68-73% of the remaining gene space, being
281 conserved in lineages 1-3 (Figure 5A). Despite extensive variation in gene content within lineages,
282 clustering of isolates based on presence/absence variation for both putative effectors and the
283 remaining of the gene space was highly similar to clustering based on 3,868 SNPs (Supplementary file
284 13), indicating that variation in gene content and SNP allelic variation reflect similar genealogical
285 processes.

286 To identify putative effectors that may be involved in host specialization of rice-infecting
287 lineages of *P. oryzae*, we first identified orthogroups with distinct patterns of presence/absence

288 across lineages. Principal component analysis of presence/absence data identified 72 orthogroups of
289 putative effectors that explained 95% of the variance of the three principal components that
290 differentiate the four lineages (PC1, PC2 and PC6; Supplementary file 13; Figure 5B), and may
291 contribute to the differences in host range among lineages. Interestingly, two among them, AvrRmg8
292 (=OG0011611) and PWL3 (=OG0011928), are host range determinants in wheat-infecting *P. oryzae*
293 since they trigger immunity in wheat varieties carrying the resistance genes *Rmg8* (Anh *et al.* 2018) or
294 *PWT3* (Inoue *et al.* 2017; Kang *et al.* 1995).

295 As host specialization can also involve sequence divergence at effector proteins, we also
296 scanned the corresponding genes for signatures of diversifying selection, i.e. an excess of non-
297 synonymous nucleotide diversity (ratio of non-synonymous to synonymous nucleotide diversity π_N/π_S
298 >1). We identified 185 orthogroups with $\pi_N/\pi_S > 1$ in at least one lineage, including 164 orthogroups
299 with $\pi_N/\pi_S > 1$ in only one lineage (lineage 1: 131 orthogroups; lineage 2: 18; lineage 3: 10; lineage 4:
300 5), and twelve, seven and two orthogroups with $\pi_N/\pi_S > 1$ in two, three or four lineages, respectively
301 (Supplementary file 14). None of these orthogroups corresponded to effectors previously
302 characterized as being involved in *P. oryzae* virulence against rice or other *Poaceae* hosts.

303 **Geographic and climatic differentiation in the distribution of *P. oryzae* lineages**

304 Our tests of adaptation to host and temperature under controlled conditions showed that
305 specialization was not strict, but it remained possible that fitness differences between lineages would
306 be sufficient under natural conditions to induce separation in different ecological niches, and/or that
307 our experimental conditions did not capture the full extent of the phenotypic differences. Here, we
308 tested the hypothesis that lineages thrive in geographically and/or environmentally different
309 conditions, which would provide indirect evidence for specialization to different habitats. We tested
310 this hypothesis by collecting geographic and climatic data for all isolates, approximating to regions or
311 the nearest cities when the exact GPS position of the sampling area was not available (Supplementary
312 file 1). At a larger scale, clonal lineages 2 and 3 were both widespread, with lineage 2 found on all

313 continents, and lineage 3 on all continents except Europe. Lineage 2 was the only lineage sampled in
314 Europe (with the exception of a single isolate from lineage 1), whereas lineage 3 was more
315 widespread in intertropical regions. Lineage 4 was mostly found in South Asia (India, Bangladesh,
316 Nepal), and in the USA and Africa (Benin, Tanzania). The recombining lineage, lineage 1, was found in
317 all continents, but was mostly found in Asia (79% of all isolates and 94% of all genotypes). At a
318 smaller scale, two, or even three different lineages were sampled in the same year in the same city in
319 11 different countries from all continents. However, in only one instance did two isolates from
320 different lineages have identical GPS positions (isolates US0106 and US0107 sampled from the same
321 field). Thus, lineages had different, but partially overlapping distributions, including some overlap
322 with the distribution of the sexually reproducing lineage (lineage 1).

323 We then investigated whether differences in the geographic range of lineages were
324 associated with differences in climatic variables. By plotting sampling locations onto a map of the
325 major climate regions (Kottek *et al.* 2006) we were able to identify clear differences in the climatic
326 distributions of lineages 2 and 3, with lineage 2 mostly found in warm temperate climates and lineage
327 3 found in equatorial climates (Figure 6; Source code 1). We used the outlying mean index (OMI),
328 which measures the distance between the mean habitat conditions used by a lineage and the mean
329 habitat conditions used by the entire species, to test the hypothesis that different lineages are
330 distributed in regions with different climates. Using information for 19 climatic variables (biomes)
331 from the WorldClim bioclimatic variables database (Fick & Hijmans 2017) for all sampling locations,
332 we obtained statistically significant results, in a permutation test on OMI values, for lineages 2, 3 and
333 4 (Source code 2; permutation test: lineage 1: OMI=2.14, $p=0.620$; lineage 2: OMI=6.54, $p<0.001$;
334 lineage 3: OMI=2.08, $p<0.001$; lineage 4: OMI=13.73, $p=0.017$). The OMI analysis, in which the first
335 two axes accounted for 69% and 25% of the variability, respectively, revealed that lineage 2 was more
336 frequent in regions with a high annual temperature range (biome 7) or a high degree of seasonality
337 (biome 4); lineage 4 was associated with regions with high levels of seasonal precipitation (biomes
338 13, 16 and 18), and lineage 3 was more frequent in regions with high temperatures (biomes 1, 6, 10

339 and 11) and high levels of isothermality (biome 3), characteristic of tropical climates (Source code 2;
340 Figure 6; Supplementary file 15).

341

342 **DISCUSSION**

343 We describe here the population structure of the rice blast fungus, and the eco-evolutionary factors
344 underlying the emergence and maintenance of multiple divergent lineages in this widespread
345 pathogen. Our analysis of SNP genotyping data showed that *P. oryzae* could be subdivided into four
346 lineages. Two of the lineages previously detected in an analysis of whole-genome data, and
347 represented by only a few individuals (lineages 5 and 6; (Gladieux *et al.* 2018b)), were assigned to
348 lineage 1 in our analysis, and may correspond to a subdivision of lineage 1. Differences in the number
349 of lineages detected may reflect an ascertainment bias, given that our SNP-genotyping beadchip was
350 designed with a set of genomic sequences that include few representatives of lineages 5 and 6.
351 Alternatively, the sampling used in the previous study (Gladieux *et al.* 2018b) may not have been
352 dense enough to reveal the lack of differentiation between lineages 1, 5 and 6, making them appear
353 to be different entities. Consistent with previous findings, our analysis of the genealogical
354 relationships between isolates revealed three clonal groups connected by long branches to a central
355 recombining group. The finding of an internationally distributed cluster in lineage 1 sheds light on the
356 early evolutionary changes contributing to the emergence of clonal lineages in this pathogen. The
357 *International* cluster of lineage 1 displayed genetic footprints of recombination and sexual
358 reproduction (in the form of an excess of homoplasious variants or relatively balanced mating types),
359 but the signal of recombination detected here may be purely historical, because we also found that
360 the clonal fraction and the frequency of sterile females were very high in this cluster. The loss of
361 female fertility may, therefore, be an early and major cause of the shift towards asexual reproduction.
362 Some genotypes assigned to the international cluster of lineage 1 may, in the future, come to
363 resemble other clonal lineages in analyses of genealogical relationships, and form a long branch
364 stemming from the central lineage 1, particularly for genotypes already displaying clonal propagation,

365 such as genotypes 2, 18, 58, 98 and 254. However, according to the principle of competitive
366 exclusion, competition between clonal lineages should only allow hegemonic expansion of the most
367 competitive clonal groups, unless they separate into different ecological niches. It may be this process
368 that ultimately leads to the fixation of a single mating type, as in clonal lineages 2-4.

369 We found that female sterility and intrinsic genetic incompatibilities represented strong
370 barriers to gene flow between the clonal lineages, potentially accounting for their maintenance over
371 time, without fusion, despite the compatibility of mating-types (at least between lineages 2 and 4
372 [*Mat1.1*] on the one hand, and lineage 3 [*Mat1.2*] on the other). These barriers to gene flow may
373 have contributed to the establishment of lineage specialization (because reproductive isolation
374 facilitates adaptation by limiting the flow of detrimental ancestral alleles in populations adapting to a
375 new habitat), accounting for the maintenance of the clonal lineages on the same host species, when
376 faced with competitive exclusion. Our analyses also show that, despite widely overlapping large-scale
377 distributions, the different lineages are essentially found in different regions, with different climatic
378 characteristics, when their distributions are observed at a finer scale. Lineage 1 was mostly sampled
379 in Southeast Asia, lineage 4 predominated in India, and lineages 2 and 3 had global distributions, but
380 the geographic ranges of all these lineages overlapped. However, an analysis of climatic data
381 indicated that lineage 2 predominated in temperate climates, where temperate japonica rice is
382 grown, lineage 3 predominated in tropical climates, in which indica rice is grown, and lineage 4
383 predominated in regions with high levels of seasonal precipitation in which the indica and aromatic
384 rice types are the principal rice types grown. Despite the finding of separation in different climatic
385 regions, our experiments revealed no strong differences between lineages in terms of sporulation
386 and mycelial growth on synthetic media at different temperatures. This suggests that, if adaptation to
387 temperature occurs in this pathogen, it was not measured by our experiments, either because it
388 involves traits other than sporulation and hyphal growth, or because the *in vitro* conditions were not
389 suitable to demonstrate differences. The host range varied across lineages, but all host ranges
390 overlapped, indicating that host specialization was not strict, or was not fully captured by our

391 experiments. Adaptation to the host may, nevertheless, decrease gene flow between populations
392 even further. For instance, lineage 2 had a narrow host range, potentially limiting the opportunities
393 for encounters and mating with other groups.

394 Effector repertoires play a key role in pathogen specialization, in fungal pathogens in general
395 (Schulze-Lefert & Panstruga 2011), and *P. oryzae* in particular (Asuke *et al.* 2020; Couch *et al.* 2005;
396 Liao *et al.* 2016; Sweigard *et al.* 1995; Takabayashi *et al.* 2002). Previous work suggested that clonal
397 lineages of *P. oryzae* possess smaller effector repertoires (Latorre *et al.* 2020) and that the clonal
398 lineage associated with japonica rice (lineage 2) possess more effectors, and in particular Avr-
399 effectors, than other clonal lineages (Latorre *et al.* 2020; Liao *et al.* 2016). Our analyzes on a larger
400 set of putative effectors (ca. 2000 in our study, vs 13 Avr-effectors in (Liao *et al.* 2016) and 178
401 known and candidate effectors in (Latorre *et al.* 2020)) confirm this trend, since lineage 2 associated
402 with temperate japonica exhibits significantly more putative effectors than lineage 3 associated with
403 indica. However, the number of non-effector genes is also greater in lineage 2 than in lineage 3, and
404 thus it remains possible that the larger effector complement of lineage 2 is a mere consequence of a
405 larger number of genes. Besides differences between lineages in richness of putative effector
406 repertoires, we show that patterns of presence / absence variation mirror patterns of population
407 subdivision based on SNP allelic variation, and thus that the differential sorting of both nucleotide
408 polymorphism and gene content across lineages reflect similar genealogical processes. Our
409 multivariate analyzes identify 72 effectors that most strongly contribute to the differentiation of the
410 4 lineages in terms of presence / absence. It is possible that the frequency differences observed at
411 these 72 effectors were due to chance events during bottlenecks at the onset of lineage formation,
412 or alternatively that their differential loss was important for the initial adaptation of lineages to new
413 rice populations or subspecies. Nucleotide diversity at synonymous and non-synonymous sites also
414 identify 185 effectors with signatures of diversifying selection in one or more lineage, possibly
415 mediated by coevolutionary interactions with host molecules. In the future, it will be interesting to

416 determine the molecular targets of these effectors and decipher the relationship between their
417 polymorphism and their mode of action.

418 Our results also indicate that lineage 1 may pose a major threat to rice production. Most
419 effectors with signature of diversifying selection were identified in lineage 1, highlighting the higher
420 ability of this lineage to rapidly fix advantageous mutations. Eleven of the 12 most multivirulent
421 isolates (lesion type > 2 on more than 40 varieties tested) belonged to lineage 1, and the *Yule* cluster,
422 in particular, was highly pathogenic on indica varieties. The propagation of such highly pathogenic
423 genotypes, belonging to a lineage that has both mating types and fertile females, should be
424 monitored closely. The monitoring of lineage 1 is all the more critical because this lineage has an
425 intermediate geoclimatic distribution that overlaps largely with the distributions of the other three
426 lineages, and some of the attempted crosses between clonal lineage 2-4 isolates and recombining
427 lineage 1 isolates produced viable progeny. This finding confirms the possibility of gene flow into this
428 lineage, as previously demonstrated on the basis of admixture mapping (Gladieux *et al.* 2018b), but it
429 also raises the question of the threat posed by gene flow from lineage 1, which is highly pathogenic,
430 to the other lineages.

431 In conclusion, our study of genetic and phenotypic variation within and between clonal
432 lineages, and within the recombinant lineage of *P. oryzae* suggests a scenario for the emergence of
433 widespread clonal lineages. The loss of female fertility may be a potent driver of the emergence of
434 asexually reproducing groups of clones. The reproductive isolation generated by the loss of sex and
435 the accumulation of mutations due to the absence of sexual purging would facilitate the
436 specialization of some of these clonal groups, leading to the competitive exclusion of the least
437 efficient clonal groups, and, finally, to the propagation of clonal lineages fixed for a single mating
438 type. Our results, thus, demonstrate that the spread of a pathogen across heterogeneous habitats
439 and divergent populations of a crop species can lead to niche separation and incipient speciation in
440 the pathogen.

441

442 **MATERIALS AND METHODS**

443 **Biological material**

444 We chose 886 *P. oryzae* isolates collected on Asian rice between 1954 and 2014 as representative of
445 the global genetic diversity of the fungus. Isolates were selected on the basis of microsatellite data, to
446 maximize the number of multilocus genotypes represented ((Saleh *et al.* 2014) and unpublished
447 data), or based on geographic origin in the absence of genotypic data, to maximize the number of
448 countries represented in the dataset.

449

450 Sixty-eight isolates were selected for experimental measurements of reproductive success,
451 adaptation to host, and growth and sporulation experiments at different temperatures
452 (Supplementary file 1). This subset of isolates included 10 isolates from each of the three clonal
453 lineages (lineages 2-4), 27 isolates from the various clusters within lineage 1 [*Baoshan* (9 isolates),
454 *International* (10), *Laos* (8), and *Yule* (11)].

455

456 Forty-four varieties were chosen as representative of the five main genetic subgroups of
457 Asian rice (Garris *et al.* 2005): indica (Chau, Chiem chanh, DA11, De abril, IR8, JC120, Pappaku), aus
458 (Arc 10177, Baran boro, Black gora, DA8, Dholi boro, Dular, FR13 A, JC148, Jhona 26, Jhona 149,
459 Kalamkati, T1, Tchampa, Tepi boro), temperate japonica (Aichi asahi, Kaw luyoeng, Leung pratew,
460 Maratelli, Nep hoa vang, Nipponbare, Sariceltik, Som Cau 70A), tropical japonica (Azucena,
461 Binulawan, Canella de ferro, Dholi boro, Gogo lempuk, Gotak gatik, Trembese) and aromatic (Arc
462 10497, Basmati lamo, Dom zard, Firooz, JC1, Kaukkyisaw, N12). The Maratelli (temperate japonica)
463 and CO39 (indica) varieties were used as susceptible controls.

464

465 **Genotyping**

466 *Pyricularia oryzae* isolates were genotyped at 5,657 genomic positions with an Illumina Infinium
467 beadchip microarray carrying single-nucleotide polymorphisms identified in 49 genomes of rice- and
468 barley-infecting *P. oryzae* isolates previously characterized (Gladieux et al., 2018b). The final dataset
469 included 3,686 biallelic SNPs without missing data.

470

471 **Whole genome sequencing**

472 Twenty-nine isolates were sequenced using Illumina HiSeq 3000 (Supplementary file 10). Isolates
473 were grown on rice flour-agar medium for mycelium regeneration, then in liquid rice flour medium
474 (Adreit *et al.* 2007). Genomic DNA extraction was carried out using >100 mg of fresh mycelium from
475 liquid culture. Fresh mycelium dried on Miracloth paper was crushed in liquid nitrogen. Nucleic acids
476 were subsequently extracted using an extraction buffer (2 % CTAB – 1.4 M NaCl – 0.1 M Tris-HCl pH 8
477 – 20 mM EDTA pH 8 added before use with 1 % final of Na₂SO₃), then purified with a
478 chloroform:isoamyl alcohol 24:1 treatment, precipitated overnight in isopropanol, and rinsed with 70%
479 ethanol. The extracted nucleic acids were further treated with Rnase A (0.2mg/mL final) and purified
480 with another chloroform:isoamyl alcohol 24:1 treatment followed by an overnight ethanol
481 precipitation. The concentration of extracted genomic DNA was assessed on Qubit® using the dsDNA
482 HS Assay Kit. The purity of extracted DNA was checked by verifying that the 260/280 and 260/230
483 absorbance ratios measured with NanoDrop were between 1.8 and 2.0. Preparation of TruSeq nano
484 libraries and HiSeq3000 sequencing (150 nucleotide reads, and 500 bp insert size) was carried out at
485 GeT-PlaGe (INRAE, Toulouse, France).

486

487 **Genome assembly, gene prediction, orthology analysis, effector prediction, and summary statistics** 488 **of nucleotide variation**

489 For the 123 sequenced isolates included in the dataset, low-quality reads were removed using the
490 software CUTADAPT (Martin 2011). Reads were assembled using ABYSS 2.2.3 (Jackman *et al.* 2017;

491 Simpson *et al.* 2009) using different K-mer sizes and for each isolate we chose the assembled
492 sequence with the highest N50 for further analyses. Genes were predicted with BRAKER 2.1.5 (Hoff *et*
493 *al.* 2015; Hoff *et al.* 2019) using RNAseq data (Pordel *et al.* 2020) as extrinsic evidence for model
494 refinement. Genes were also predicted with AUGUSTUS 3.4.0 (Stanke & Morgenstern 2005)(training
495 set=*Magnaporthe grisea*) and gene models that did not overlap with gene models identified with
496 BRAKER were added to the GFF file generated with the latter. Repeated regions were masked using
497 REPEATMASKER 4.1.0 (<http://www.repeatmasker.org/>). The completeness of genome assemblies and
498 gene predictions was assessed using BUSCO (Simão *et al.* 2015), and completeness in BUSCO genes
499 was greater than 93.7% (Supplementary file 10). Putative effector genes were identified as genes
500 encoding proteins predicted to be secreted by at least two methods among three [SIGNALP 4.1
501 (Nielsen 2017), TARGETP (Emanuelsson *et al.* 2000) and PHOBIUS (Käll *et al.* 2004)], without predicted
502 transmembrane domain based on TMHMM analysis (Krogh *et al.* 2001), without predicted motif of
503 retention in the endoplasmic reticulum based on PS-SCAN (Bhagwat & Aravind 2007), and without
504 CAZy annotation based on DBSCAN v7 (Yin *et al.* 2012). Differences in numbers of putative effectors
505 and non-effectors among lineages (ANOVA and Tukey's HSD test) were tested using using the SCIPY
506 1.6.0 package in PYTHON. Homology relationships among predicted genes were established using
507 ORTHOFINDER v2.4.0 (Emms & Kelly 2015). Principal component analysis of presence/absence
508 variation of putative effectors and non-effector proteins was carried out using R package PRCOMP. We
509 used the `get_pca_var()` in PRCOMP to extract the results for variables (i.e. effectors) and identify
510 effectors whose contribution to principal components was the greatest, defined as effectors with a
511 contribution to loadings of PC1, PC2 and PC6 greater than 1%. To estimate the numbers of core and
512 accessory genes, we used a rarefaction approach to account for differences in sample size across
513 lineages. For each pseudo-sample size, we estimated the size of the core and accessory genome in
514 each lineage using a maximum of 2000 pseudosamples. Sequences for each orthogroup were aligned
515 and cleaned with TRANSLATORX (Abascal *et al.* 2010) using default parameters. The ratio of non-

516 synonymous to synonymous diversity π_N/π_S was calculated for each orthogroup for lineages with
517 sample size greater than or equal to four using EGGLIB 3 (<https://www.egglib.org>).

518

519 **Population subdivision and recombination**

520 Among the 886 *P. oryzae* isolates genotyped, we identified 264 different multilocus genotypes, which
521 were used for the analysis of population subdivision. We used the sNMF program to infer individual
522 ancestry coefficients in K ancestral populations. This program is optimized for the analysis of large
523 datasets and does not assume Hardy-Weinberg equilibrium. It is, therefore, more appropriate to deal
524 with inbred or clonal lineages (Frichot *et al.* 2014) . We used SPLITSTREE version 4 (Huson & Bryant
525 2006) to visualize relationships between genotypes in a phylogenetic network, with reticulations to
526 represent the conflicting phylogenetic signals caused by homoplasy. We also used the pairwise
527 homoplasy index (PHI) test implemented in SPLITSTREE to test the null hypothesis of clonality. We used
528 the sNMF software to investigate population subdivision further within the cluster for which the null
529 hypothesis of clonality could be rejected. Weir and Cockerham's F_{ST} was calculated with the R package
530 HIERFSTAT, by the WC84 method (Goudet 2005).

531

532 **Experimental measurement of reproductive success and female fertility**

533 *Pyricularia oryzae* is a heterothallic fungus with two mating types (*Mat1.1* and *Mat1.2*). Sexual
534 reproduction between strains of opposite mating type can be observed in laboratory conditions, and
535 results in the production of ascospores within female sexual structures called perithecia (Saleh *et al.*
536 2012a). On synthetic media, perithecia are formed at the contact zone between parental mycelia.
537 Crosses were carried out on a rice flour agar medium (20 g rice flour, 2.5 g yeast extract, 15 g agar
538 and 1 L water, supplemented with 500 000 IU penicillin G after autoclaving for 20 min at 120°C), as
539 described by (Saleh *et al.* 2012a). We assessed reproductive success by determining the production of
540 perithecia produced after three weeks of culture at 20°C under continuous light. Each cross was

541 carried out twice and we computed the average number of perithecia across repeats. Perithecia can
542 be formed by the two interacting partners or by one partner only. Isolates forming perithecia are
543 described as female-fertile. We measured female fertility for 220 isolates (listed in Supplementary file
544 1), by monitoring perithecium production in crosses involving the tester strains CH0997 (Mat1.2) and
545 CH0999 (Mat1.1). We further assessed the presence of asci and germinating ascospores in perithecia
546 for a subset of crosses, by excising perithecia with a scalpel and counting the number of germinated
547 filaments for each individual ascus after overnight incubation on water agar. The subset of crosses
548 included 10 Mat1.1 isolates (lineage 1: CH0999, CH1065, CH1076; lineage 2: CH0092, MC0016,
549 SP0006; lineage 4: IN0017, IN0092, NP0070, CH0718) and 6 Mat1.2 isolates (lineage 1: CH0997;
550 CH1083, CH1120; lineage 3: BR0019, CH0549, MD0929).

551

552 **Pathogenicity tests**

553 Compatibility between *P. oryzae* isolates and rice plants from the five main genetic subgroups of rice
554 (indica, temperate japonica, tropical japonica, aus and aromatic) was measured in controlled
555 conditions. Seventy isolates were inoculated on 46 varieties. Inoculations were performed as
556 described by (Gallet *et al.* 2016). Conidial suspensions ($25\ 000\ \text{conidia.mL}^{-1}$) in 0.5% gelatin were
557 sprayed onto three-week-old rice seedlings (> 6 plants/variety). The inoculated plants were incubated
558 for 16 hours in the dark at 27°C and 100% humidity and then for seven days with a day/night
559 alternation (13 hours at 27°C/11 hours at 21°C), before scoring symptoms. Lesion type was rated from
560 1 to 6 (Gallet *et al.* 2016) and the symptom type was assessed visually on leaves. Each interaction was
561 assessed in three independent experiments, and the maximum of the three scores was used in
562 calculations.

563

564 **Mycelial growth and sporulation rate at different temperatures**

565 Mycelial growth and sporulation rate were measured for 41 isolates at five different temperatures
566 (10°C, 15°C, 20°C, 25°C and 30°C). For each isolate, Petri dishes containing PDA medium were
567 inoculated with mycelial plugs placed at the center, and incubated in a growth chamber with a fixed
568 temperature. Mycelium diameter was estimated as the average of two measurements made along
569 two perpendicular axes at different time points. At the end of the experiment, conidia were collected
570 by adding 5 mL of water supplemented with 0.01% Tween 20 to the Petri dish and rubbing the
571 surface of the mycelium. Conidia were counted with a hemocytometer. Three or four independent
572 experiments were performed for each isolate, at each temperature. We had initially planned to carry
573 out only three independent experiments. However, because some isolates did not grow in the first
574 experiment, and because some cultures were invaded by mites and had to be discarded in the second
575 and third experiment, a fourth experiment was eventually performed for some temperature
576 conditions.

577

578 **Statistical analyses of climatic and phenotypic data**

579 Ecological niche separation: OMI (outlying mean index), or marginality, is used to study niche
580 separation and niche breadth. OMI gives the same weight to all samplings, whether rich or poor in
581 species and individuals, and is particularly suitable in cases in which sampling is not homogeneous.
582 OMI measures the deviation between the mean environmental conditions used by one lineage and
583 the mean environmental conditions used by all lineages. OMI analysis then places the lineages in
584 environmental conditions maximizing their OMI. Environmental values, consisting of 19 biome values
585 (WorldClim bioclimatic variables (Fick & Hijmans 2017)), were retrieved for all sampling locations.
586 Climatic values were normalized before the analysis. A contingency table was generated to associate
587 the number of isolates from each lineage with each sampling location. Only isolates with a precise
588 location (known region, city or GPS position of sampling) were included. A random permutation test,
589 with 10000 permutations, was used to assess the statistical significance of marginality for each
590 lineage.

591 Pathotyping: Ordinal symptoms scores were analyzed with a proportional-odds model
592 accounting for ordered categorical responses with a `clm()` function implemented in the ordinal R
593 package (version 2018.8-25). The significance of the factors was analyzed by ANOVA. Pairwise
594 comparisons of significant factors were performed after computing least-squares means with LSMEANS
595 version 2.30-0 in R, with Tukey adjustment.

596 Mycelium growth: Mycelium growth was analyzed separately for each temperature, with a
597 linear mixed-effects model. The significance of the factors was analyzed by ANOVA. Post-hoc pairwise
598 comparisons were performed after computing least-squares means with LSMEANS version 2.30-0 in R.

599 Sporulation: The median number of spores calculated for the various repetitions of the
600 experiment was analyzed with a Kruskal-Wallis test. Post-hoc pairwise comparisons were performed
601 using Dunn's non-parametric multiple comparison test.

602

603 **ACKNOWLEDGMENT**

604 We thank Tatiana Giraud for useful suggestions. We thank all our colleagues who shared strains or
605 participated in the collection of rice blast samples.

606

607

608 **REFERENCES**

- 609 Abascal F, Zardoya R, Telford MJ (2010) TranslatorX: multiple alignment of nucleotide sequences
610 guided by amino acid translations. *Nucleic Acids Research* **38**, W7-W13.
- 611 Abbate JL, Gladieux P, Hood ME, *et al.* (2018) Co-occurrence among three divergent plant-castrating
612 fungi in the same *Silene* host species. *Molecular ecology* **27**, 3357-3370.
- 613 Adreit H, Santoso, Andriantsimalona D, *et al.* (2007) Microsatellite markers for population studies of
614 the rice blast fungus, *Magnaporthe grisea*. *Molecular Ecology Notes* **7**, 667-670.
- 615 Ali S, Gladieux P, Leconte M, *et al.* (2014) Origin, migration routes and worldwide population genetic
616 structure of the wheat yellow rust pathogen *Puccinia striiformis* f. sp. *tritici*. *PLoS pathogens*
617 **10**, e1003903.
- 618 Anh VL, Inoue Y, Asuke S, *et al.* (2018) Rmg8 and Rmg7, wheat genes for resistance to the wheat blast
619 fungus, recognize the same avirulence gene AVR-Rmg8. *Molecular Plant Pathology* **19**, 1252-
620 1256.

- 621 Asuke S, Tanaka M, Hyon G-S, *et al.* (2020) Evolution of an Eleusine-specific subgroup of *Pyricularia*
622 *oryzae* through a gain of an avirulence gene. *Molecular Plant-Microbe Interactions* **33**, 153-
623 165.
- 624 Bhagwat M, Aravind L (2007) Psi-blast tutorial. In: *Comparative genomics*, pp. 177-186. Springer.
- 625 Bueker B, Eberlein C, Gladieux P, *et al.* (2016) Distribution and population structure of the anther
626 smut *Microbotryum silenes-acaulis* parasitizing an arctic-alpine plant. *Molecular ecology* **25**,
627 811-824.
- 628 Burdon JJ (1993) The structure of pathogen populations in natural plant communities. *Annual review*
629 *of phytopathology* **31**, 305-323.
- 630 Couch BC, Fudal I, Lebrun M-H, *et al.* (2005) Origins of Host-Specific Populations of the Blast
631 Pathogen *Magnaporthe oryzae* in Crop Domestication With Subsequent Expansion of
632 Pandemic Clones on Rice and Weeds of Rice. *Genetics* **170**, 613-630.
- 633 Emanuelsson O, Nielsen H, Brunak S, Von Heijne G (2000) Predicting subcellular localization of
634 proteins based on their N-terminal amino acid sequence. *Journal of molecular biology* **300**,
635 1005-1016.
- 636 Emms DM, Kelly S (2015) OrthoFinder: solving fundamental biases in whole genome comparisons
637 dramatically improves orthogroup inference accuracy. *Genome Biology* **16**, 157.
- 638 Fick SE, Hijmans RJ (2017) WorldClim 2: new 1-km spatial resolution climate surfaces for global land
639 areas. *International journal of climatology* **37**, 4302-4315.
- 640 Frichot E, Mathieu F, Trouillon T, Bouchard G, François O (2014) Fast and efficient estimation of
641 individual ancestry coefficients. *Genetics* **196**, 973-983.
- 642 Gallet R, Fontaine C, Bonnot F, *et al.* (2016) Evolution of compatibility range in the rice-
643 *magnaporthe oryzae* system: an uneven distribution of R genes between rice subspecies.
644 *Phytopathology* **106**, 348-354.
- 645 Garris AJ, Tai TH, Coburn J, Kresovich S, McCouch S (2005) Genetic structure and diversity in *Oryza*
646 *sativa* L. *Genetics* **169**, 1631-1638.
- 647 Gibson AK, Hood ME, Giraud T (2012) Sibling competition arena: selfing and a competition arena can
648 combine to constitute a barrier to gene flow in sympatry. *Evolution: International Journal of*
649 *Organic Evolution* **66**, 1917-1930.
- 650 Giraud T, Gladieux P, Gavrillets S (2010) Linking the emergence of fungal plant diseases with
651 ecological speciation. *Trends in ecology & evolution* **25**, 387-395.
- 652 Giraud T, Koskella B, Laine AL (2017) Introduction: microbial local adaptation: insights from natural
653 populations, genomics and experimental evolution. *Molecular ecology* **26**, 1703-1710.
- 654 Gladieux P, Condon B, Ravel S, *et al.* (2018a) Gene Flow between Divergent Cereal- and Grass-Specific
655 Lineages of the Rice Blast Fungus *Magnaporthe oryzae*. *mBio* **9**.
- 656 Gladieux P, Guerin F, Giraud T, *et al.* (2011) Emergence of novel fungal pathogens by ecological
657 speciation: importance of the reduced viability of immigrants. *Molecular ecology* **20**, 4521-
658 4532.
- 659 Gladieux P, Ravel S, Rieux A, *et al.* (2018b) Coexistence of multiple endemic and pandemic lineages of
660 the rice blast pathogen. *MBio* **9**.
- 661 Goudet J (2005) Hierfstat, a package for R to compute and test hierarchical F-statistics. *Molecular*
662 *Ecology Notes* **5**, 184-186.
- 663 Hardin G (1960) The competitive exclusion principle. *Science* **131**, 1292-1297.
- 664 Hoff KJ, Lange S, Lomsadze A, Borodovsky M, Stanke M (2015) BRAKER1: unsupervised RNA-Seq-
665 based genome annotation with GeneMark-ET and AUGUSTUS. *Bioinformatics* **32**, 767-769.
- 666 Hoff KJ, Lomsadze A, Borodovsky M, Stanke M (2019) Whole-genome annotation with BRAKER. In:
667 *Gene Prediction*, pp. 65-95. Springer.
- 668 Huson DH, Bryant D (2006) Application of Phylogenetic Networks in Evolutionary Studies. *Molecular*
669 *Biology and Evolution* **23**, 254-267.
- 670 Inoue Y, Vy TTP, Yoshida K, *et al.* (2017) Evolution of the wheat blast fungus through functional losses
671 in a host specificity determinant. *Science* **357**, 80-83.

- 672 Jackman SD, Vandervalk BP, Mohamadi H, *et al.* (2017) ABySS 2.0: resource-efficient assembly of
673 large genomes using a Bloom filter. *Genome Research* **27**, 768-777.
- 674 Käll L, Krogh A, Sonnhammer ELL (2004) A combined transmembrane topology and signal peptide
675 prediction method. *Journal of molecular biology* **338**, 1027-1036.
- 676 Kang S, Sweigard Ja Fau - Valent B, Valent B (1995) The PWL host specificity gene family in the blast
677 fungus *Magnaporthe grisea*. *Molecular Plant Microbe Interactions*.
- 678 Kottek M, Grieser J, Beck C, Rudolf B, Rubel F (2006) World map of the Köppen-Geiger climate
679 classification updated.
- 680 Krogh A, Larsson B, Von Heijne G, Sonnhammer ELL (2001) Predicting transmembrane protein
681 topology with a hidden Markov model: application to complete genomes. *Journal of*
682 *molecular biology* **305**, 567-580.
- 683 Latorre SM, Reyes-Avila CS, Malmgren A, *et al.* (2020) Differential loss of effector genes in three
684 recently expanded pandemic clonal lineages of the rice blast fungus. *BMC biology* **18**, 1-15.
- 685 Liao J, Huang H, Meusnier I, *et al.* (2016) Pathogen effectors and plant immunity determine
686 specialization of the blast fungus to rice subspecies. *Elife* **5**, e19377.
- 687 Marin M, Preisig O, Wingfield BD, Kirisits T, Wingfield MJ (2009) Single sequence repeat markers
688 reflect diversity and geographic barriers in Eurasian populations of the conifer pathogen
689 *Ceratocystis polonica*. *Forest Pathology* **39**, 249-265.
- 690 Martin M (2011) Cutadapt removes adapter sequences from high-throughput sequencing reads.
691 *EMBnet. journal* **17**, 10-12.
- 692 Nielsen H (2017) Predicting secretory proteins with SignalP. In: *Protein function prediction*, pp. 59-73.
693 Springer.
- 694 Nosil P, Vines TH, Funk DJ (2005) Perspective: reproductive isolation caused by natural selection
695 against immigrants from divergent habitats. *Evolution; international journal of organic*
696 *evolution* **59**, 705-719.
- 697 Pagliaccia D, Urak RZ, Wong F, *et al.* (2018) Genetic structure of the rice blast pathogen
698 (*Magnaporthe oryzae*) over a decade in North Central California rice fields. *Microbial ecology*
699 **75**, 310-317.
- 700 Pordel A, Ravel S, Charriat F, *et al.* (2020) Tracing the origin and evolutionary history of *Pyricularia*
701 *oryzae* infecting maize and barnyard grass. *Phytopathology*[®], PHYTO-09.
- 702 Robert S, Zapater M-F, Carlier J, Abadie C, Ravigné V (2015) Multiple introductions and admixture at
703 the origin of the continental spread of the fungal banana pathogen *Mycosphaerella fijiensis*
704 in Central America: a statistical test using approximate Bayesian computation. *Revue*
705 *d'écologie*.
- 706 Ropars J, Lo YC, Dumas E, *et al.* (2016) Fertility depression among cheese-making *Penicillium*
707 *roqueforti* strains suggests degeneration during domestication. *Evolution; international*
708 *journal of organic evolution* **70**, 2099-2109.
- 709 Saleh D, Milazzo J, Adreit H, Fournier E, Tharreau D (2014) South-East Asia is the center of origin,
710 diversity and dispersion of the rice blast fungus, *Magnaporthe oryzae*. *New Phytologist* **201**,
711 1440-1456.
- 712 Saleh D, Milazzo J, Adreit H, Tharreau D, Fournier E (2012a) Asexual reproduction induces a rapid and
713 permanent loss of sexual reproduction capacity in the rice fungal pathogen *Magnaporthe*
714 *oryzae*: results of in vitro experimental evolution assays. *BMC evolutionary biology* **12**, 1-16.
- 715 Saleh D, Xu P, Shen Y, *et al.* (2012b) Sex at the origin: an Asian population of the rice blast fungus
716 *Magnaporthe oryzae* reproduces sexually. *Molecular ecology* **21**, 1330-1344.
- 717 Schulze-Lefert P, Panstruga R (2011) A molecular evolutionary concept connecting nonhost
718 resistance, pathogen host range, and pathogen speciation. *Trends in plant science* **16**, 117-
719 125.
- 720 Servedio MR, Van Doorn GS, Kopp M, Frame AM, Nosil P (2011) Magic traits in speciation: 'magic' but
721 not rare? *Trends in ecology & evolution* **26**, 389-397.

- 722 Simão FA, Waterhouse RM, Ioannidis P, Kriventseva EV, Zdobnov EM (2015) BUSCO: assessing
723 genome assembly and annotation completeness with single-copy orthologs. *Bioinformatics*
724 **31**, 3210-3212.
- 725 Simpson JT, Wong K, Jackman SD, *et al.* (2009) ABySS: a parallel assembler for short read sequence
726 data. *Genome Research* **19**, 1117-1123.
- 727 Stanke M, Morgenstern B (2005) AUGUSTUS: a web server for gene prediction in eukaryotes that
728 allows user-defined constraints. *Nucleic Acids Research* **33**, W465-W467.
- 729 Sweigard JA, Carroll AM, Kang S, *et al.* (1995) Identification, Cloning, and Characterization of
730 *PWL2*, a Gene for Host Species Specificity in the Rice Blast Fungus. *Plant Cell* **7**, 1221-
731 1233.
- 732 Takabayashi N, Tosa Y, Oh HS, Mayama S (2002) A Gene-for-Gene Relationship Underlying the
733 Species-Specific Parasitism of *Avena/Triticum* Isolates of *Magnaporthe grisea* on Wheat
734 Cultivars. *Phytopathology* **92**, 1182-1188.
- 735 Taylor JW, Fisher MC (2003) Fungal multilocus sequence typing—it's not just for bacteria. *Current*
736 *opinion in microbiology* **6**, 351-356.
- 737 Taylor JW, Turner E, Townsend JP, Dettman JR, Jacobson D (2006) Eukaryotic microbes, species
738 recognition and the geographic limits of species: examples from the kingdom Fungi.
739 *Philosophical Transactions of the Royal Society B: Biological Sciences* **361**, 1947-1963.
- 740 Tharreau D, Fudal I, Andriantsimialona D, *et al.* (2009) World population structure and migration of
741 the rice blast fungus, *Magnaporthe oryzae*. In: *Advances in genetics, genomics and control of*
742 *rice blast disease*, pp. 209-215. Springer.
- 743 Walker A, Gladieux P, Decognet V, *et al.* (2015) Population structure and temporal maintenance of
744 the multihost fungal pathogen *Botrytis cinerea*: causes and implications for disease
745 management. *Environmental microbiology* **17**, 1261-1274.
- 746 Yang N, Ma G, Chen K, Wu X (2018) The population genetics of *Alternaria tenuissima* in four regions
747 of China as determined by microsatellite markers obtained by transcriptome sequencing.
748 *Frontiers in microbiology* **9**, 2904.
- 749 Yin Y, Mao X, Yang J, *et al.* (2012) dbCAN: a web resource for automated carbohydrate-active enzyme
750 annotation. *Nucleic Acids Research* **40**, W445-W451.
- 751 Yoshida K, Saunders DGO, Mitsuoka C, *et al.* (2016) Host specialization of the blast fungus
752 *Magnaporthe oryzae* is associated with dynamic gain and loss of genes linked to transposable
753 elements. *Bmc Genomics* **17**, 1.
- 754 Zhong Z, Chen M, Lin L, *et al.* (2018) Population genomic analysis of the rice blast fungus reveals
755 specific events associated with expansion of three main clades. *The ISME journal* **12**, 1867-
756 1878.

757

758 DATA AVAILABILITY

759 All raw sequencing data are deposited under accession code PRJEB42377.

760

761 The following data sets were generated:

762 1. European Nucleotide Archive

763 M Thierry, F Charriat, J Milazzo, H Adreit, S Ravel, S Cros-Arteil, S Borron, V Sella, T Kroj, R Ioos, E Fournier, D Tharreau, P
764 Gladieux

765 ID PRJEB42377 Whole genome sequencing of *Pyricularia oryzae* fungi isolated from rice.

766 2. Zenodo

767 M Thierry, F Charriat, J Milazzo, H Adreit, S Ravel, S Cros-Arteil, S Borron, V Sella, T Kroj, R loos, E Fournier, D Tharreau, P
768 Gladieux
769 Single-nucleotide polymorphisms, genome assemblies, genome annotations, and gene predictions of *Pyricularia oryzae*
770 isolates from rice
771 doi 10.5281/zenodo.4561581
772

773 The following previously published data sets were used:

774 1. European Nucleotide Archive

775 A Pordel, S Ravel, F Charriat, P Gladieux, S Cros-Arteil, J Milazzo, H Adreit, M Javan-Nikkhah, A Mirzadi-Gohari, A Moumeni,
776 D Tharreau
777 ID PRJEB41186 Origin and evolutionary history of *Pyricularia oryzae* fungal pathogens infecting maize and barnyard grass in
778 Iran

779
780 2. European Nucleotide Archive

781 Z Zhong, M Chen, L Lin, Y Han, J Bao, W Tang, L Lin, Y Lin, R Somai, L Lu, W Zhang, J Chen, Y Hong, X Chen, B Wang, WC Shen,
782 G Lu, J Norvinyeku, DJ Ebbola, Z Wang
783 ID PRJNA354675 Population Genomic Analysis of the Rice Blast Fungus Reveals Specific Events Associated With Expansion
784 of Three Main Clades

785

786 **ADDITIONAL FILES**

787 **Source code 1.** R code used to prepare maps in Figure 6.

788 **Source code 2.** R code used for analyses based on the Outlying Mean Index, including Principal Component
789 Analysis presented in Figure 6.

790 **Supplementary file 1.** Isolates of *Pyricularia oryzae*

791 **Supplementary file 2.** Assignment of genotypes to clusters identified in this study, in Gladieux et al. 2018b (A)
792 and in Saleh et al. 2014 (B and C).

793 **Supplementary file 3.** F_{ST} estimates between clusters within lineage 1.

794 **Supplementary file 4.** Analysis of mycelial growth rates.

795 **Supplementary file 5.** Mycelial growth rates.

796 **Supplementary file 6.** Analysis of sporulation rates.

797 **Supplementary file 7.** Sporulation rates.

798 **Supplementary file 8.** Matrix of compatibility between four lineages of *P. oryzae* isolates and five subspecies of
799 rice plants, as determined by pathogenicity tests in controlled conditions. Numbers in the matrix represent the
800 maximum symptom score across three replicate experiments. Numbers at the right and bottom margins
801 represent the number of compatible interactions observed (symptom score >2) for varieties and isolates,
802 respectively.

803 **Supplementary file 9.** Analysis of pathogenicity data.

804 **Supplementary file 10.** Sequenced isolates.

805 **Supplementary file 11.** Violin plots showing the number of putative effectors and non-effector proteins
806 detected in each lineage. Asterisks indicate significant differences in gene content (Tukey's HSD test; $p < 0.001$).

807 **Supplementary file 12.** Estimating the size of the core and accessory genome using a rarefaction approach. For
808 each lineage, genomes were resampled in ≤ 2000 combinations of $N-1$ genomes (N being the sample size). (A)
809 Non-effector genes. (B) Putative effectors.

810 **Supplementary file 13.** Principal component analysis based on the presence/absence of accessory putative
811 effectors and non-effector proteins. Panels A and B show principal component PC1 against PC2, and PC1
812 against PC6, respectively, for effectors. Panels C and D show principal component PC1 against PC2, and PC1
813 against PC6, respectively, for non-effectors. Between parentheses is the proportion of variance represented by
814 each principal component.

815 **Supplementary file 14.** Summary statistics of non-synonymous and synonymous polymorphism in four lineages
816 of *P. oryzae*. For each lineage, only orthogroups with sample size ≥ 4 were included in calculations. Lineage:
817 lineage of origin of genomes used in calculations for each orthogroup. Orthogroup: orthogroup ID. N: sample
818 size. numNS: number of non-synonymous sites. numS: number of synonymous sites. SNS: number of non-
819 synonymous segregating sites. SS: number of synonymous segregating sites. PiNS: non-synonymous nucleotide
820 diversity. PiS: synonymous nucleotide diversity.

821 **Supplementary file 15.** ecological niches of the four major lineages (referred to as L1 to L4) considering each of
822 the 19 biomes individually (referred to as Bio1 to Bio19). The x-axis represents the outlying mean index (OMI),
823 which measures the distance between the mean habitat conditions used by a lineage and the mean habitat
824 conditions used by the entire species, to test the hypothesis that different lineages are distributed in regions
825 with different climates.

826 **Figure 1 – source data 1.** Multilocus genotypes for neighbor-net phylogenetic inference.

827 **Figure 1 – source data 2.** Ancestry proportions in $K=4$ sNMF clusters.

828 **Figure 2 – source data 1.** Multilocus genotypes for neighbor-net phylogenetic inference.

829 **Figure 2 – source data 2.** Ancestry proportions in $K=4$ sNMF clusters.

830 **Figure 2 – source data 3.** Geographic distribution of clones (i.e. multilocus genotypes repeated multiple times).

831 **Figure 3 – Source data 1.** Production of perithecia.

832 **Figure 3 – Source data 2.** Production of germinating ascospores

833 **Figure 4 – source data 1.** Symptom scores for *P. oryzae* isolates inoculated onto rice varieties

834 **Figure 5 – source data 1.** Size of core and accessory genomes for putative effectors and non-effector proteins

835 **Figure 5 – source data 2.** Presence and absence of putative effectors in *P. oryzae* genomes

836 **Figure 6 – source data 1.** GPS position of isolates

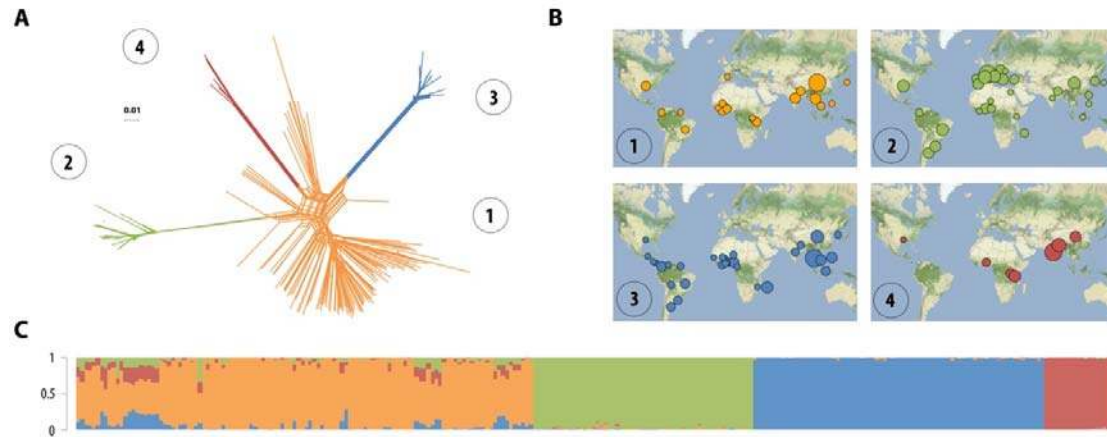


Figure 1. Rice-infecting *P. oryzae* populations are divided into four major lineages. Population subdivision was inferred from 264 distinct *P. oryzae* genotypes, representing 886 isolates, and the four lineages were represented in different colors. A: Neighbor-net phylogenetic network estimated with SPLITSTREE; reticulations indicate phylogenetic conflicts caused by homoplasy. B: Geographic distribution of the four lineages identified with SPLITSTREE and sNMF, with disk area proportional to sample size. C: Ancestry proportions in $K=4$ clusters, as estimated with sNMF software; each multilocus genotype is represented by a vertical bar divided into four segments indicating membership in $K=4$ clusters.

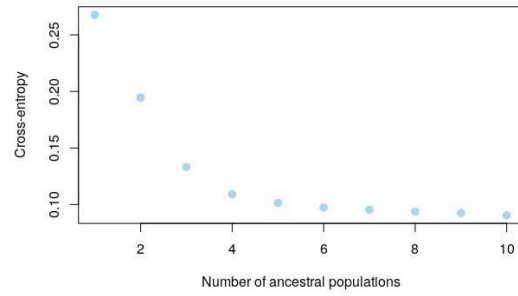


Figure 1 – figure supplement 1. Cross-entropy (CE) as a function of the number of clusters K modeled in sNMF analyses of population subdivision.

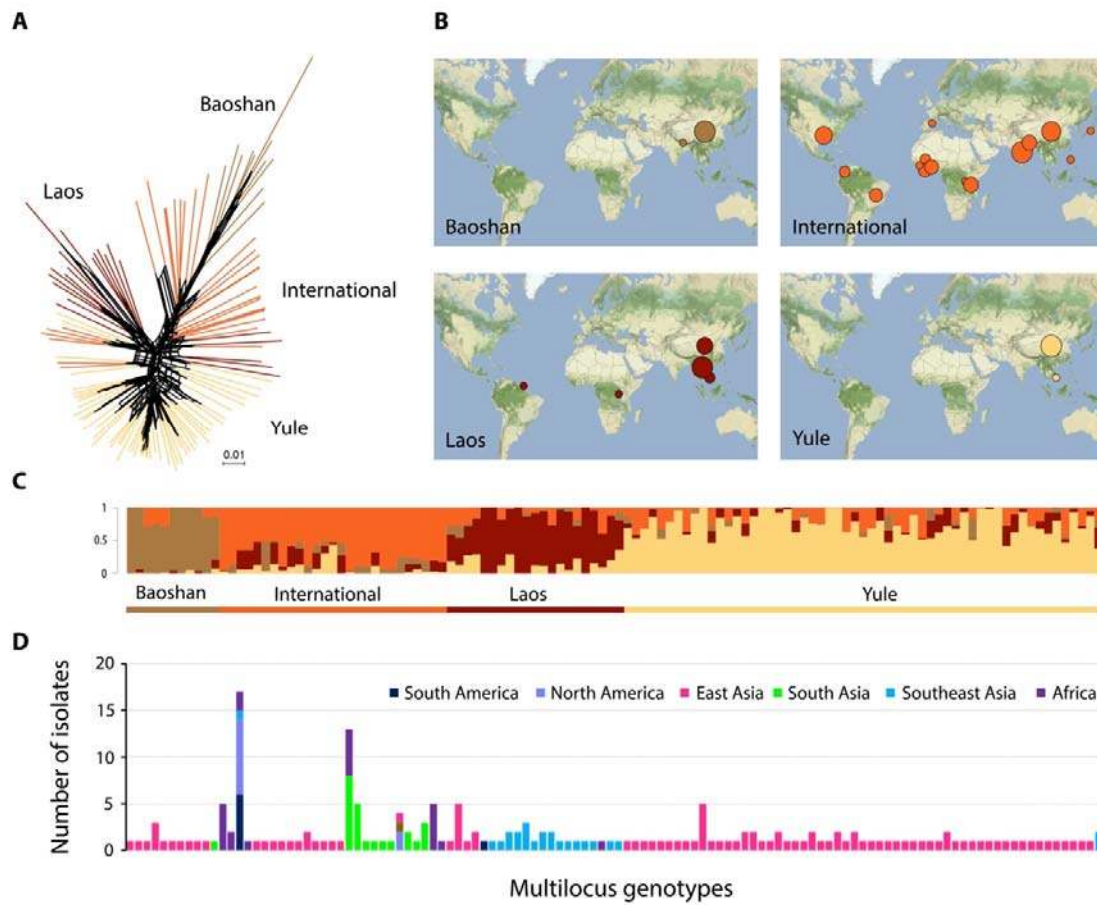
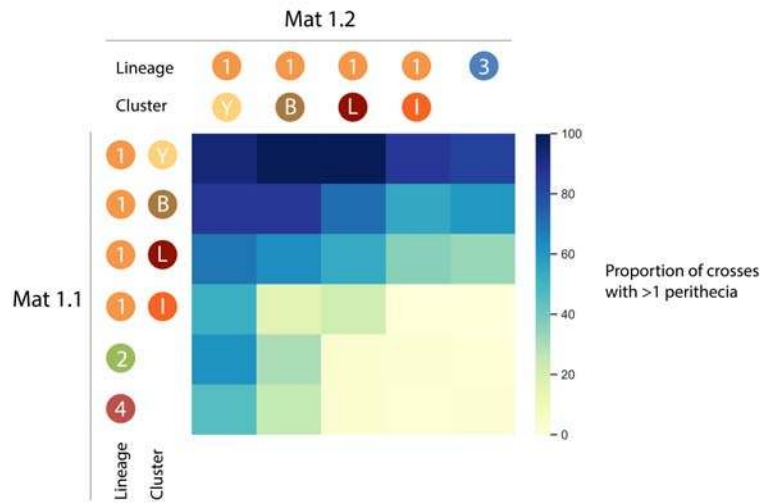


Figure 2. Population subdivision in lineage 1. A: Neighbor-net phylogenetic network estimated with SPLITSTREE; reticulations indicate phylogenetic conflicts caused by homoplasy. B: Geographic distribution of the four clusters identified with sNMF, with disk area proportional to number of isolates. C: Ancestry proportions in four clusters, as estimated with sNMF; each multilocus genotype is represented by a vertical bar divided into four segments, indicating membership in $K=4$ clusters. D: Number of isolates and their geographic origin for each multilocus genotype of lineage 1. Panels C and D share an x-axis (each vertical bar represents a different multilocus genotype).

(A) Production of perithecia



(B) Production of germinating ascospores

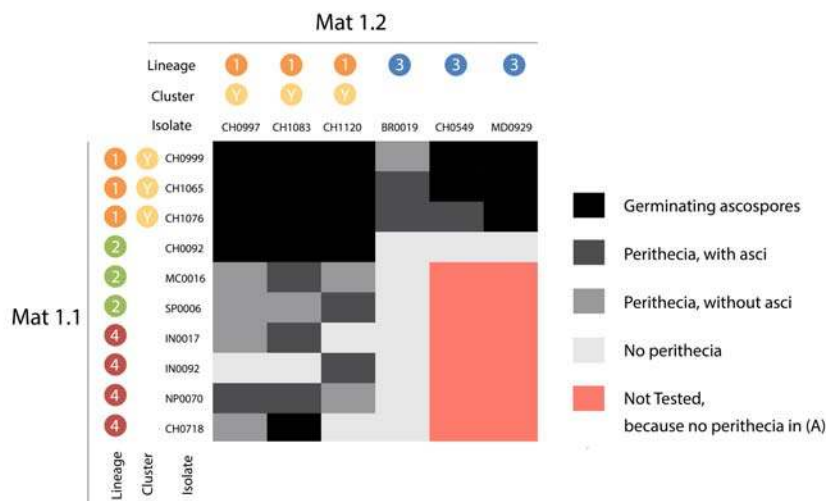


Figure 3. Success of crosses between lineages 2-4 and clusters within lineage 1 with (A) proportion of crosses producing at least one perithecia, (B) scoring of ascus formation and ascospore germination for a subset of crosses.

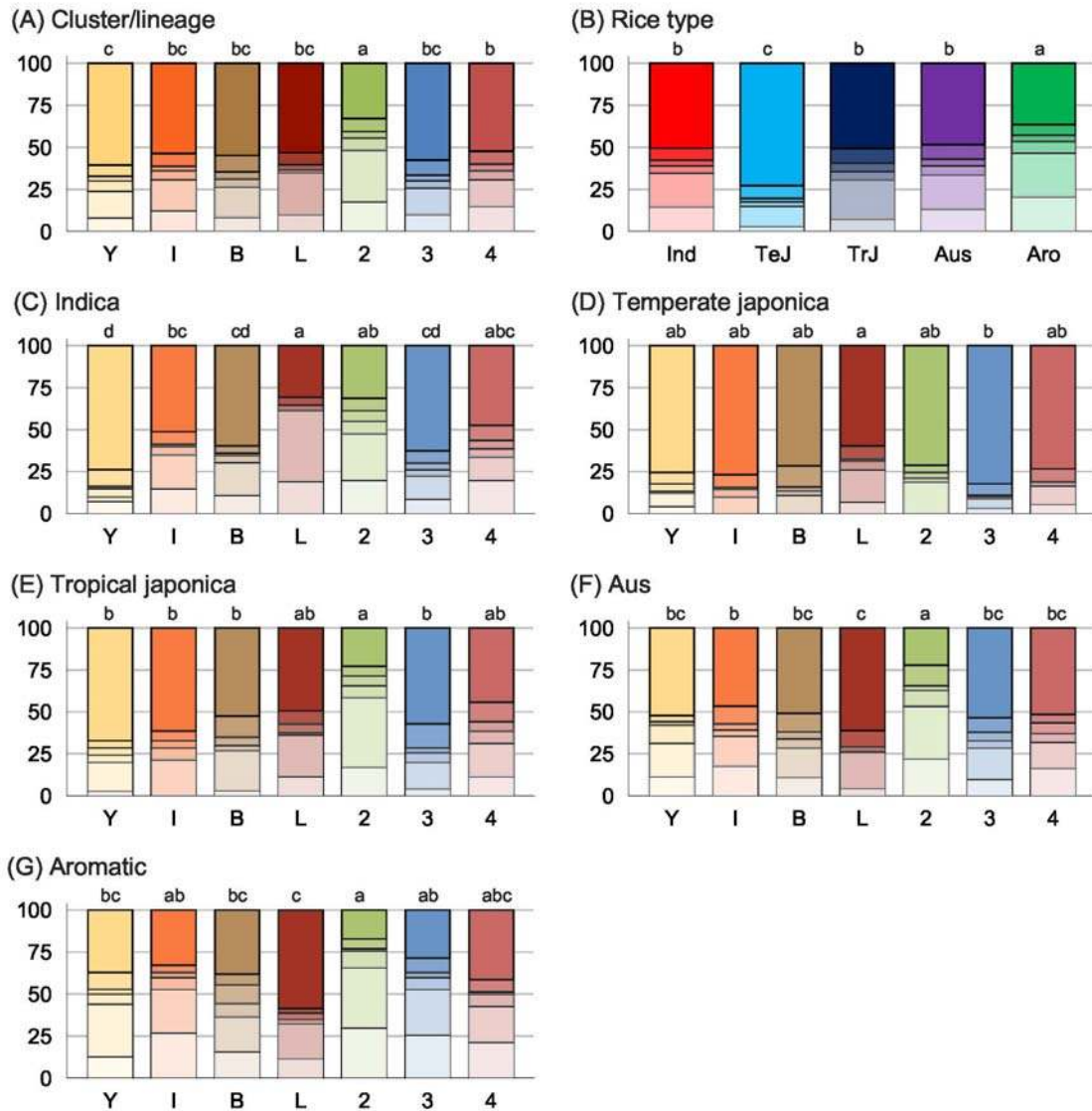


Figure 4: Compatibility between 70 *P. oryzae* isolates and 44 rice varieties, representing five types of rice. A: Proportions of symptom scores as a function of the lineage of origin of isolates, or cluster of origin for isolates from lineage 1; B: Proportions of symptom scores as a function of the type of rice; C-G: Proportions of symptom scores as a function of the lineage of origin of isolates, for each type of rice. Abbreviations: Y, *Yule*; I, *International*; B, *Baoshan*; L, *Laos*; 2, lineage 2; 3, lineage 3; 4, lineage 4; Ind, indica; TeJ, temperate japonica; TrJ, tropical japonica; Aro, aromatic. Small capitals indicate significant differences. All interactions were assessed in three independent experiments, and the highest of the three symptom scores was used in calculations.

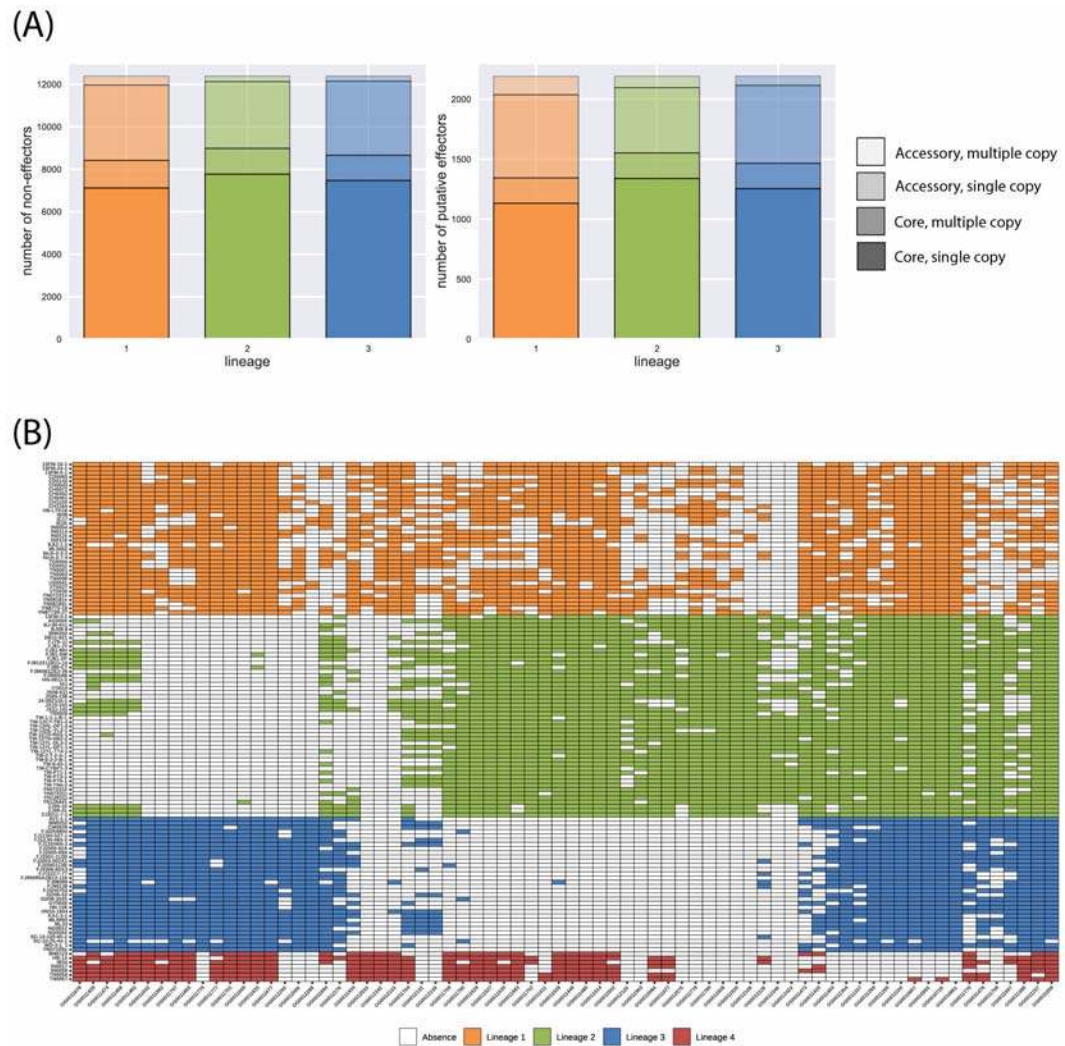


Figure 5. Pangenome analyses of 123 genomes of *P. oryzae*, representing four rice-infecting lineages. (A) Size of core and accessory genomes for putative effectors and non-effector proteins estimated using a rarefaction approach with a pseudo-sample size of $n=30$ genomes. Lineage 4 was not included due to small sample size. (B) Presence and absence in lineage 1-4 of the 72 putative effectors with the highest contribution to principal components 1, 2 and 6, in a principal component analysis of presence/absence data (Supplementary file 13).

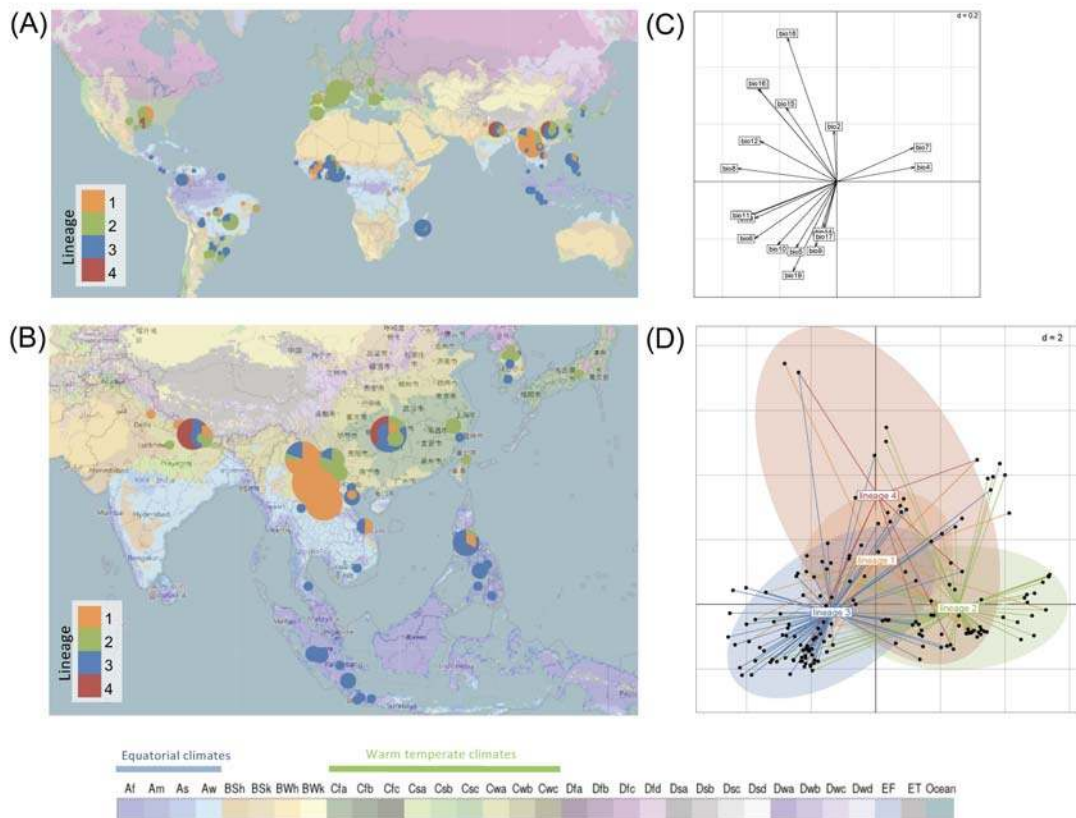


Figure 6. Geographic distribution of four lineages of *P. oryzae* and corresponding climatic data. (A, B) Pie charts representing the distribution of the four lineages in the world (A) and in South, East and Southeast Asia (B), keeping only isolates for which the sampling position was precisely known (i.e., for which the region, city or GPS position was documented). Background map is from OpenStreetMap (CC-BY-SA) and represents the updated Köppen-Geiger climate classification of main climates at world scale as described in (Kottek *et al.* 2006). (C, D) Outlying Mean Index analysis, testing the separation of ecological niches among lineages, with (C) canonical weights of the 19 environmental variables included in the analysis, and (D) site coordinates (dots) and realized niches of lineages represented as ellipses. Variable bio13 co-localizes with bio16, and variables bio1 and bio3 co-localize with bio11. The 11 temperate variables included in the analysis were (bio1) Annual Mean Temperature, (bio2) Mean Diurnal Range, (bio3) Isothermality [$100 \cdot (\text{bio2}/\text{bio7})$], (bio4) Temperature Seasonality [standard deviation*100], (bio5) Max Temperature of Warmest Month, (bio6) Min Temperature of Coldest Month, (bio7) Temperature Annual Range [bio5-bio6], (bio8) Mean Temperature of Wettest Quarter, (bio9) Mean Temperature of Driest Quarter, (bio10) Mean Temperature of Warmest Quarter, (bio11) Mean Temperature of Coldest Quarter. The 8 precipitation variables included in the analysis were (bio12) Annual Precipitation, (bio13) Precipitation of Wettest Month, (bio14) Precipitation of Driest Month, (bio15) Precipitation Seasonality (Coefficient of

Variation), (bio16) Precipitation of Wettest Quarter, (bio17) Precipitation of Driest Quarter, (bio18) Precipitation of Warmest Quarter, (bio19) Precipitation of Coldest Quarter.